

# Electronic structure of cubic $\text{ScF}_3$ from first-principles calculations

**P Zhgun<sup>1</sup>, D Bocharov<sup>1,2,3</sup>, S Piskunov<sup>1,2,3</sup>, A Kuzmin<sup>3</sup> and J Purans<sup>3</sup>**

<sup>1</sup> Faculty of Physics and Mathematics, University of Latvia, Zellu Str. 8, LV-1002 Riga, Latvia

<sup>2</sup> Faculty of Computing, University of Latvia, Raina Blvd. 19, LV-1586 Riga, Latvia

<sup>3</sup> Institute of Solid State Physics, University of Latvia, Kengaraga Str. 8, LV-1063 Riga, Latvia

E-mail: pjotr.zgun@gmail.com

**Abstract.** The first-principles calculations have been performed to investigate the ground state properties of cubic scandium trifluoride ( $\text{ScF}_3$ ) perovskite. Using modified hybrid exchange-correlation functionals within the density functional theory (DFT) we have comprehensively compared the electronic properties of  $\text{ScF}_3$  obtained by means of the linear combination of atomic orbitals (LCAO) and projector augmented-waves (PAW) methods. Both methods allowed us to reproduce the lattice constant experimentally observed in cubic  $\text{ScF}_3$  at low temperatures and predict its electronic structure in good agreement with known experimental valence-band photoelectron and F 1s X-ray absorption spectra.

## 1. Introduction

Scandium trifluoride ( $\text{ScF}_3$ ) is a promising material attracted much attention due to recently discovered strong negative thermal expansion (NTE) coefficient over a wide range of temperatures from 10 to 1100 K [1].

At atmospheric pressure  $\text{ScF}_3$  has cubic (space group  $Pm\bar{3}m$ )  $\text{ReO}_3$ -type structure (Fig. 1) down to at least 10 K [1]. However, opposite to the metallic  $\text{ReO}_3$ , which has very weak NTE effect [2, 3], scandium trifluoride is an insulator with band gap of more than 8 eV [4]. A cubic-to-rhombohedral phase transition occurs in  $\text{ScF}_3$  at high pressure ( $P>0.5$  GPa at  $T\sim 300$  K or  $P=0.1\text{--}0.2$  GPa at 50 K) as determined from X-ray and neutron diffraction studies [1, 5]. Raman spectroscopy confirms that upon pressure increase cubic  $\text{ScF}_3$  undergo a phase transition to the rhombohedral (space group  $R\bar{3}c$ ) phase [5, 6].

The electronic structure of  $\text{ScF}_3$  thin films has been investigated by means of resonant photoemission spectroscopy at the Sc 2p and F 1s absorption edges in Ref. [4]. Two charge-transfer-type satellites, the first one at about 13 eV below the main peaks in the valence-band and the second one with an energy separation of about 9–10 eV, were observed and indicate the strong hybridization effect between Sc 3d and F 2p states [4].

The phonon properties of  $\text{ScF}_3$  have been studied using a combination of inelastic neutron scattering experiment with *ab initio* calculations of lattice dynamics [7]. It was shown that a description of NTE within the quasi-harmonic approximation is not reliable in the case of  $\text{ScF}_3$ . The authors in [7] have demonstrated that the  $R4+$  mode (the one with the lowest energy at  $R$ -point of Brillouin zone (BZ)) has quartic potential and proposed the mechanism for NTE based on this anharmonicity. The transition between the ground state and the first excited

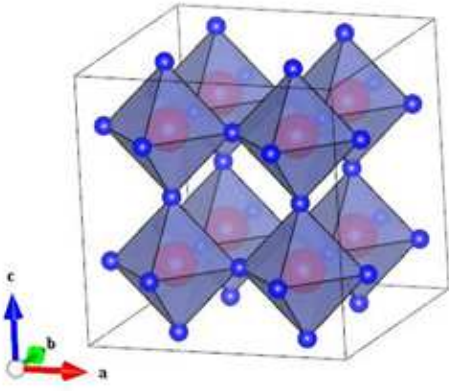


**Figure 1.** Schematic view of cubic  $\text{ScF}_3$  structure (space group  $Pm\bar{3}m$ ) built up of  $\text{ScF}_6$  regular octahedra joined by corners (small balls are fluorine atoms, large balls are scandium atoms). All  $\text{Sc}-\text{F}-\text{Sc}$  angles are equal to  $180^\circ$ .

state ( $\sim 19$  meV) of the  $R4+$  mode has been associated with experimentally observed phonon peak ( $\sim 25$  meV), which stiffens upon increasing temperature [7].

In spite of mainly experimental efforts have been performed to understand the NTE in  $\text{ScF}_3$ , its origin is still under debate. Therefore, comprehensive theoretical study is necessary to elucidate the nature of this peculiar property. In this study we report the results of *ab initio* electronic structure calculations for cubic  $\text{ScF}_3$  using the linear combination of atomic orbitals (LCAO) and projector augmented-waves (PAW) methods.

## 2. Computational details

In this study  $\text{ScF}_3$  is modeled by means of two different methods: (i) LCAO within the framework of hybrid density functional approach and (ii) PAW calculations using the generalized gradient approximation (GGA) density functional.

To perform hybrid LCAO calculations, we used the periodic CRYSTAL09 code [8], which employs Gaussian-type functions centered on atomic nuclei as the basis set for expansion of the crystalline orbitals. The full-electron basis sets used in this study for F and Sc were taken from CRYSTAL basis set library [8]. Threshold parameters for evaluation of different types of bielectronic integrals such as overlap and penetration tolerances for Coulomb integrals, overlap tolerance for exchange integrals and pseudo-overlap tolerances for exchange integral series [8] have been set to  $10^{-8}$ ,  $10^{-8}$ ,  $10^{-8}$ ,  $10^{-8}$  and  $10^{-16}$ , respectively. Calculations are considered as converged when the total energy obtained in the self-consistent field procedure differs by less than  $10^{-10}$  a.u. in the two successive cycles.

LCAO calculations of  $\text{ScF}_3$  have been performed using a set of hybrid Hartree-Fock/Kohn-Sham (HF/KS) exchange-correlation functionals [9, 10, 11, 12, 13] combining exact HF nonlocal exchange and KS exchange operator within the GGA as implemented in the CRYSTAL09 code [8]. We have constructed the following hybrid functionals: “BECKE & LYP”, “BECKE & PWGGA”, “PBE & PBE”, “PBEsol & PBEsol”, where the first terms refer to the KS exchange and the second terms to the KS correlation parts of a hybrid functional, while the weight of the HF exchange has been varied for each functional separately between 0 and 100%.

DFT calculations using the PAW method as implemented in the VASP code [14] were performed for comparison. We have compared PW91 [13] and PBE [9] exchange-correlation potentials as well as large-core effective core potential (LC-ECP) with three  $3d^14s^2$  valence electrons and small-core effective core potential (SC-ECP) with eleven  $3s^23p^63d^14s^2$  valence electrons for Sc atom. Fluorine atom for all calculations was described as ECP with  $2s^22p^5$  valence shell. Hybrid HF-DFT calculations have been also performed with the weight of exact HF exchange part equal to 25%. The optimal cut-off energy has been equal to 1000 eV.

To provide the balanced summation over the direct and reciprocal lattices of  $\text{ScF}_3$  in both

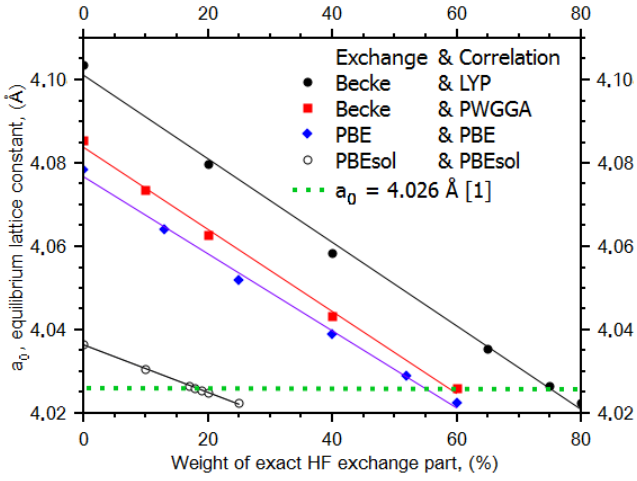


**Figure 2.** Equilibrium lattice constant with respect to the weight of exact HF non-local exchange in hybrid density calculation by means of the LCAO method.

LCAO and PAW methods, the reciprocal space integration has been performed by sampling the BZ with the  $8 \times 8 \times 8$  Pack-Monkhorst  $k$ -mesh [15] that results in 35 eventually distributed  $k$ -points in the irreducible BZ.

### 3. Choice of exchange-correlation functional

The influence of the exchange-correlation functional type and the weight ( $w_{\text{HF}}$ ) of exact HF non-local exchange in hybrid density calculations within the LCAO method on the lattice parameter in  $\text{ScF}_3$  is shown in Fig. 2. We found that pure GGA functionals overestimate the experimental value of lattice constant  $a_0=4.026$  Å [1], while stepwise increase of the  $w_{\text{HF}}$  for about 10% leads to proportional decrease of  $a_0$  by approximately  $-0.01$  Å. The PBESol functional with  $w_{\text{HF}}=18\%$  reproduces perfectly the experimental lattice parameter and has been selected for further calculations.

Values of the lattice constant  $a_0$  obtained using pure GGA calculations by the VASP code [14] are in the range of  $4.02$ – $4.03$  Å if LC-ECP is used for Sc, while  $a_0$  of  $4.06$ – $4.07$  Å has been obtained if SC-ECP has been adopted for Sc. Using hybrid HF-DFT calculations with the PBE0 functional [14]), the value of  $a_0$  is equal to  $\sim 4.04$ – $4.05$  Å: it is larger when LC-ECP is used for Sc and is smaller when SC-ECP is used.

To additionally justify the choice of hybrid functional, we have calculated the value of the band gap ( $E_g$ ). Until now the band gap of  $\text{ScF}_3$  was not precisely measured experimentally, but it is estimated to be larger than 7–8 eV [4]. All hybrid functionals constructed for LCAO method ( $w_{\text{HF}}$  corresponds to  $a_0=4.026$  Å, see Fig. 2) show that  $\text{ScF}_3$  is an insulator with relatively large band gap  $E_g > 8$  eV. In the PAW GGA calculations the band gap is underestimated as it is predicted by the theory for pure GGA functionals: it is equal to 5.5–6.0 eV. Hybrid PAW calculations allowed us to obtain  $E_g$  equal to 8–9 eV, which is closer to the experimental estimate.

Thus, for electronic structure calculations we have finally chosen the “PBESol & PBESol” functional with  $w_{\text{HF}}=18\%$ , giving  $E_g=9.8$  eV, for LCAO method and the PW91 functional with  $w_{\text{HF}}=25\%$ , giving  $E_g=8.9$  eV, for PAW method.

### 4. Electronic properties

The effective charges of scandium and fluorine atoms were calculated using Mulliken population analysis [8] in LCAO method and Bader topological analysis [16] in PAW calculations. The LCAO charges are equal to  $q_{\text{Sc}}=+2.28\text{e}$  and  $q_{\text{F}}=-0.76\text{e}$ . In PAW method the atom charges were slightly different for two Sc pseudopotentials:  $q_{\text{Sc}}=+2.70\text{e}$  and  $q_{\text{F}}=-0.90\text{e}$  for LC-ECP and

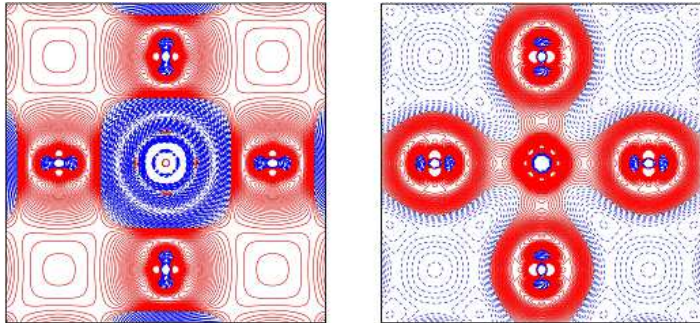


**Figure 3.** Plots of the charge density difference in (100) plane between the full charge density of crystal and electronic density of non-interacting atoms (left panel) and ions (right panel) obtained using “PBEsol & PBEsol” functional with  $w\text{HF} = 18\%$ . Solid (red) and dashed (blue) isolines correspond to positive (excess) and negative (deficiency) electron density difference, respectively.

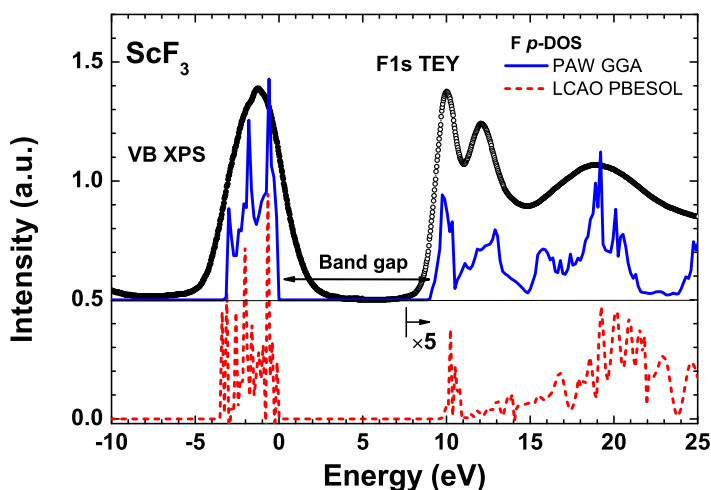


**Figure 4.** A comparison of the  $\text{F } p$  density of states (DOS) calculated by means of the LCAO (dashed line) and PAW (solid line) methods with valence-band photoelectron [17] and  $\text{F } 1s$  X-ray absorption spectra [4]. The amplitude of the DOS in the conduction band was multiplied by a factor of 5. Energy scale is given with respect to the calculated top of the valence band. Experimental spectra has been aligned to match best the calculations.

$q_{\text{Sc}}=+2.17\text{e}$  and  $q_{\text{F}}=-0.73\text{e}$  for SC-ECP. These results demonstrate a considerable deviation of effective atomic charges from formal charges caused by partly covalent nature of  $\text{Sc}-\text{F}$  bonds.

Fig. 3 shows electron density maps in (100) plane of  $\text{ScF}_3$  obtained using LCAO calculation as a difference between the full charge density of crystal and electronic density of non-interacting atoms or ions. The anisotropy of electron density induced by bond covalent contribution is clearly visible in both graphs: the electron density is larger along the crystallographic axes.

In Fig. 4 we compare the partial  $\text{F } p$  density of states (DOS) calculated by both LCAO and PAW methods with the experimental valence-band (VB) photoelectron spectrum taken from Ref. [17] and the  $\text{F } 1s$  X-ray absorption spectrum taken from Ref. [4]. The VB photoelectron spectrum of  $\text{ScF}_3$  has a complex shape composed of the main peak and the shoulder located at the left side, which originate due to the valence band splitting upon hybridization of the  $\text{F } 2p$  and  $\text{Sc } 3d$  states [17]. Our theoretical calculations confirm such interpretation and reproduce well the width and asymmetric shape of the valence band. The  $\text{F } 1s$  absorption spectrum [4] consists of three well visible peaks at 9.3, 11.4 and 18.2 eV due to transitions from the  $\text{F } 1s$  core state to the  $\text{F } np$  states in the conduction band and above. The first two peaks correspond to the  $\text{F } 2p$  states in the conduction band, which are hybridized with the  $\text{Sc } 3d$  states. The two peaks originate from the  $t_{2g}-e_g$  splitting of the  $\text{Sc } 3d$  states by the octahedral crystal field. The third peak at 18.2 eV corresponds to the interaction of the  $\text{F } 2p$  and  $\text{Sc } 4p$  states. Such interpretation

is fully supported by the calculated F  $p$  DOS: in fact, good agreement with the F 1s absorption spectrum indicates that a relaxation of the electron states due to the F 1s core-hole is weak in ScF<sub>3</sub>.

## 5. Conclusions

The lattice constant, band gap and electronic properties of cubic ScF<sub>3</sub> were calculated using LCAO and PAW DFT computational methods. It was shown that a variation of exact HF exchange part allowed us to reproduce experimental value of the lattice constant  $a_0=4.026$  Å [1].

The band gap obtained in hybrid HF-DFT calculations is equal to 8–10 eV and agree well with the expected value [4]. A deviation of atom charges from formal ones and an anisotropy of electronic density point to the covalent nature of Sc–F bonds in ScF<sub>3</sub>. Calculated partial F  $p$  DOS is in a good agreement with valence-band photoelectron [17] and F 1s X-ray absorption [4] spectra.

Good agreement between the theory and available experimental data makes promising the application of the present approach to the investigation of phonon properties in ScF<sub>3</sub> in the future work.

## Acknowledgments

Authors are greatly indebted to R.A. Evarestov, D. Gryaznov, V. Kashcheyevs and A.I. Popov for many stimulating discussions. This work was supported by ESF Projects 2009/0202/1DP/1.1.2.0/09/APIA/VIAA/141 and 2009/0216/1DP/1.1.1.2.0/09/APIA/VIAA/044 and scholarship ESS2011/78/MS/6 within 2009/0162/1DP/1.1.2.1.1/09/IPIA/VIAA/004.

## References

- [1] Greve B K, Martin K L, Lee P L, Chupas P J, Chapman K W and Wilkinson A P 2010 *J. Am. Chem. Soc.* **132** 15496
- [2] Chatterji T, Henry P F, Mittal R and Chaplot S L 2008 *Phys. Rev. B* **78** 134105
- [3] Rodriguez E E, Llobet A, Proffen T, Melot B C, Seshadri R, Littlewood P B and Cheetham A K 2009 *J. Appl. Phys.* **105** 114901
- [4] Umeda M, Tezuka Y, Shin S and Yagishita A 1996 *Phys. Rev. B* **53** 1783
- [5] Aleksandrov K S, Voronov N V, Vtyurin A N, Krylov A S, Molokeev M S, Oreshonkov A S, Goryainov S V, Likhacheva A Yu and Anchakov A I 2011 *Phys. Solid State* **53** 564
- [6] Aleksandrov K S, Voronov N V, Vtyurin A N, Goryainov S V, Zamkova N G, Zinenko V I and Krylov A S 2002 *J. Exper. Theor. Phys.* **94** 977
- [7] Li C W, Tang X, Muñoz J A, Keith J B, Tracy S J, Abernathy D L and Fultz B 2011 *Phys. Rev. Lett.* **107** 195504
- [8] Dovesi R, Saunders V R, Roetti C, Orlando R, Zicovich-Wilson C M, Pascale F, Civalleri B, Doll K, Harrison N M, Bush I J, D'Arco Ph and Llunell M 2009 *CRYSTAL09 User's Manual* (Torino: University of Torino) <http://www.crystal.unito.it/>
- [9] Perdew J P, Burke K and Ernzerhof M 1996 *Phys. Rev. Lett.* **77** 3865
- [10] Perdew J P, Ruzsinszky A, Csonka G I, Vydrov O A, Scuseria G E, Constantin L A, Zhou X and Burke K 2008 *Phys. Rev. Lett.* **100** 136406
- [11] Lee C, Yang W, and Parr R G 1988 *Phys. Rev. B* **37** 785
- [12] Becke A D 1988 *Phys. Rev. A* **38** 3098
- [13] Perdew J P, Chevary J A, Vosko S H, Jackson K A, Pederson M R, Singh D J and Fiolhais C 1992 *Phys. Rev. B* **46** 6671
- [14] Kresse G, Marsman M and Furthmüller J 2012 *VASP the GUIDE* (Wien: University of Wien) <http://cms.mpi.univie.ac.at/VASP/>
- [15] Monkhorst H J and Pack J D 1976 *Phys. Rev. B* **13** 5188
- [16] Bader R F W 1990 *Atoms in Molecules, A Quantum Theory* (Oxford: Oxford University Press)
- [17] Shin S, Tezuka Y, Ishii T and Ueda Y 1993 *Solid State Commun.* **87** 1051